Journal of Quantitative Spectroscopy & Radiative Transfer 121 (2013) 69–77

Contents lists available at SciVerse ScienceDirect

Journal of Quantitative Spectroscopy & Radiative Transfer

journal homepage: www.elsevier.com/locate/jqsrt

Statistical analysis of single-track instrument sampling in spaceborne aerosol remote sensing for climate research

Igor Geogdzhayev [a,b,*], Brian Cairns [b], Mikhail Alexandrov [a,b], Michael I. Mishchenko [b]

[a] Columbia University, 2880 Broadway, NY 10025, USA
[b] NASA Goddard Institute for Space Studies, 2880 Broadway, NY 10025, USA

ARTICLE INFO

Article history:
Received 18 June 2012
Received in revised form
19 September 2012
Accepted 6 February 2013
Available online 14 February 2013

Keywords:
Tropospheric aerosols
Satellite remote sensing
Climate change
Aerosol climatology
Long-term variability

ABSTRACT

We examine likely effects of pixel-wide along-track sampling on climatological means of aerosol optical thickness (AOT) derived from observations with satellite instruments such as CALIOP and APS by sub-sampling AOT retrievals from a wide-swath imaging instrument (MODIS). The advantage of using daily pixel-level aerosol retrievals from MODIS rather than aerosol transport models to assess the results of along-track sampling is that limitations caused by the presence of clouds are implicit in the satellite dataset, so that their seasonal and regional variations are captured coherently. However, imager data can exhibit latitudinal (cross-track) variability of monthly global mean AOTs caused by a scattering-angle dependence. This makes it difficult to separate natural variability from viewing-geometry artifacts complicating direct comparisons of an along-track sub-sample with the full imager data. To work around this problem, we introduce "latitudinal-track" sampling which, by design, captures the cross-track AOT variability of the original imager data. We show that the latitudinal-track standard error of global monthly mean AOTs is much smaller than the longitudinal-track one. This allows us to attribute the difference between the two errors to MODIS viewing-geometry artifacts and obtain an upper limit on AOT errors caused by along-track sampling. We conclude that single-track instruments provide AOT sampling sufficient for climate applications. Since AOT is believed to be the most variable characteristic of tropospheric aerosols, our results imply that pixel-wide along-track coverage also provides adequate statistical representation of the global distribution of aerosol microphysical parameters.

1. Introduction

Tropospheric aerosols contribute to climate change via direct and indirect effects, but the magnitude of this contribution and even its sign remain uncertain [1–6]. Satellite observations are expected to provide the climate community with important constrains on the global distribution of the amount and microphysics of aerosols with the goal of improving modeling accuracy and gaining educated insights into aerosol chemistry and transport.

In terms of their spatial coverage of tropospheric aerosols, satellite instruments can be classified into two categories: imagers (such as the MODerate resolution Imaging Spectroradiometer (MODIS) [7–9], the Multi-angle Imaging SpectroRadiometer (MISR) [10–12], and POLarization and Directionality of the Earth's Reflectance instrument (POLDER) [13]) and along-track sensors (such as the Cloud-Aerosol LIdar with Orthogonal Polarization (CALIOP) [14] and Aerosol Polarimetry Sensor (APS) [15,16]). The two instrument classes are complementary from the standpoint of their scientific objectives. The frequency and density of sampling of imagers are essential for observing

* Corresponding author at: Columbia University, 2880 Broadway, NY 10025, USA. Tel.: +1 212 678 5511; fax: +1 212 678 5552.
E-mail address: igor.v.geogdzhayev@nasa.gov (I. Geogdzhayev).

0022-4073/$ - see front matter
http://dx.doi.org/10.1016/j.jqsrt.2013.02.003

small-scale or rapidly evolving aerosol events and facilitate comparisons with ground-based and *in situ* measurements. On the other hand, specialized capabilities (such as high-accuracy polarization channels with on-board calibration, wide spectral range, and a dense grid of angular views) of along-track passive sensors (e.g., APS) and active lidars (e.g., CALIOP) make them highly sensitive to aerosol microphysics (APS, [16,17]) or aerosol vertical distribution (CALIOP [14]). This complementarity motivated the inclusion of instruments of both types in the A-train formation.

The minimal set of retrieval requirements for the Glory APS was formulated and discussed in Refs. [15,18]. It is based on the overall objective to create an advanced global climatology of detailed aerosol and cloud properties that would serve the immediate needs of the modeling and climate communities. It is, therefore, important to know to what extent the reduced sampling of along-track instruments such as CALIOP and APS affects the statistical accuracy of a satellite climatology of retrieved aerosol properties. The way to accomplish this task adopted in this paper is to study the statistics of pixel-wide subsets of daily imager retrievas. The MODIS level 2 aerosol dataset is an instructive choice for this study because this instrument has a wide swath yielding global coverage every 1 or 2 days. The MODIS aerosol optical thickness (AOT) data have been thoroughly characterized (e.g., [19–28]), in particular by comparing them with ground-based AErosol RObotic NETwork (AERONET; [29,30]) measurements, and have been widely used in aerosol research.

2. Data

For our analysis, we use MODIS Terra collection 5 level 2 AOT retrievals separately over land and ocean. Since AOT is believed to be the most variable aerosol parameter, one can expect the magnitude of sampling artifacts inferred from the analysis of spatial AOT distributions to be the upper limit of those for other aerosol characteristics (such as size, shape, real and imaginary refractive index, etc.). We consider the period from 2001 to 2007. Only retrievals with quality flag values exceeding 0 (over ocean) or equal to 3 (over land) were used. The data have a native resolution at nadir of 10 km. For simplicity, in this paper we will refer to these individual aerosol retrievals as MODIS pixels. They should not be confused with the original detector radiance measurements with a 500 m resolution at nadir. Each cross-track scan consists of 135 pixels and can therefore be averaged to any grid spacing coarser than 10 km. A 10° grid size was chosen here to yield a regional spatial average (cf. Ref. [31]) sufficient to sample the direct radiative forcing with adequate spatial resolution [32].

We limit the geographic latitude of the retrievals to be between 60°S and 60°N. We then accumulate three groups of subsets of MODIS pixels monthly on the 10° by 10° grid as follows.

- The first group is a single dataset composed of all available MODIS pixels. It can be referred to as the “full imager data”.

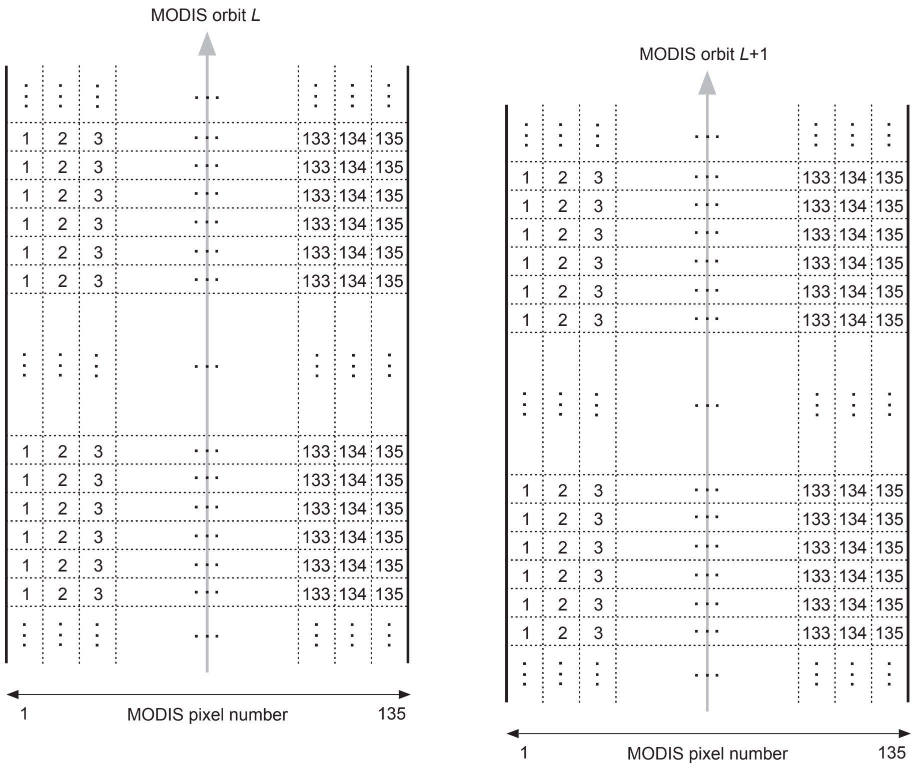

Fig. 1. The diagram shows MODIS swaths corresponding to two consecutive MODIS orbits and explains the partitioning of all level-2 MODIS AOT data into 135 sets corresponding to individual longitudinal tracks parallel to the MODIS ground track. The rows represent MODIS cross-track scans consisting of 135 aerosol pixels each. The number in each cell indicates the set (or, equivalently, the longitudinal track) to which the pixel is attributed.

- The second group is comprised of 135 sets, each containing only pixels corresponding to a specific MODIS longitudinal track number (Fig. 1). These sets may be thought of as being produced by 135 virtual along-track instruments, each collecting its own data and simulating the pixel-wide along-track spatial sampling of a CALIOP- or APS-like instrument.
- The third group consists of 135 sets of data obtained by dividing all MODIS cross-track scans into sequential 135-scan segments, numbering cross-track scans in each segment by assigning numbers between 1 and 135, and retaining in each set only the pixels with a specific scan number from all segments (Fig. 2). This third group emulates 135 so-called "latitudinal-track" instruments that make measurements by scanning perpendicularly to the satellite vector of motion the same way MODIS does. However, each of them is "turned on" only for a short period of time to collect just one cross-track scan of MODIS data from each 135-scan segment.

Note that here we use the terms "longitudinal" and "latitudinal" to describe tracks of MODIS data, respectively, parallel and perpendicular to the satellite vector of motion. Given that the orbit inclination of the Terra satellite is 98.2°, these tracks are not aligned with the geographic meridians and latitudes.

The rationale for considering the above virtual instruments is as follows. MODIS has a cross-track swath of 2330 km and follows an orbit with a repeat cycle of 16 days, each day yielding between ~26,000 and ~28,000 cross-track scans. Let us consider the results that a virtual longitudinal-track and a latititudinal-track instrument would produce globally on the time scale of a month under the idealized assumption that the MODIS AOT dataset has no retrieval errors. Since both instruments subsample the same global AOT field constituting the original imager data, we may expect their respective AOT means to deviate from the full-imager means by a similar amount. This is because the sizes of the subsamples that these virtual instruments produce are nearly the same and are distributed uniformly around the globe. The variability of the means generated by the virtual instruments would in this case be defined only by the natural variability of aerosols. The number of MODIS longitudinal tracks (135) and the necessity to have subsamples of equal size determines the choice of the number of latitudinal tracks, but the choice of a scan number between 1 and 135 is arbitrary, which makes the latitudinal-track datasets thus obtained statistically equivalent. In order to make sure that no artifacts are introduced due to an unlikely correlation between a given latitudinal-track sample and a latitude location, we ran a test in which the along-track extent of the MODIS granules was reduced to 191 (a prime number) from its normal value of around 203. No statistically significant effect of this change was found on the results presented in the next section.

3. Analysis

We thus obtained datasets of gridded monthly mean AOT values for each of the three groups introduced previously in each 10° by 10° grid cell. Global AOT values can then be calculated by averaging over all cells. By

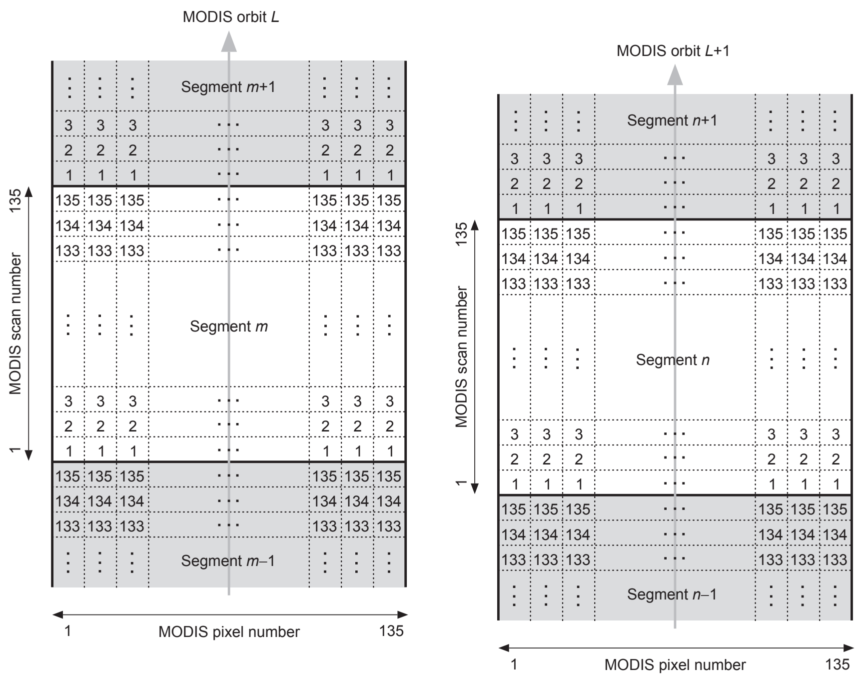

Fig. 2. The diagram shows MODIS swaths corresponding to two consecutive MODIS orbits and explains the partitioning of all level-2 MODIS AOT data into 135 sets corresponding to individual "latitudinal tracks" perpendicular to the MODIS ground track. Three consecutive 135-scan segments are shown for each swath. The number in each cell indicates the set (or, equivalently, the latitudinal track) to which the pixel is attributed.

comparing the global monthly mean values of the full imager and virtual longitudinal-track instruments, one can attempt to estimate the effects of the along-track sub-sampling for instruments such as APS. Cloudiness may affect the performance of a sampling scheme of the global aerosol field because tropospheric aerosol retrievals are difficult in presence of clouds. A sampling approach that is based on transport models and performs adequately in an idealized case of a cloudless atmosphere may fail to capture the influence of aerosol patterns masked by seasonal and regional variations of cloudiness. The advantage of using daily pixel-level aerosol retrievals from MODIS to assess the results of along-track sampling is that limitations caused by the presence of clouds are implicit in the sample, so that the seasonal and regional variations of such cloud effects are captured coherently. The only problem with using an imager to assess a pixel-wide along-track sample accuracy is that if there are any view-angle biases in the imager AOT product then these biases will increase the differences of the means from any two MODIS longitudinal tracks above the level caused by the natural variability of the aerosol field, thereby causing an overestimation of the single-track sample error. We therefore need to first analyze the potential view-angle biases.

In Fig. 3a, we show the variation of the MODIS AOT with scattering angle for the 7-year period considered. The results are presented for land and ocean for all retrievals (solid curves) and for pixels with AOTs not exceeding 0.1 (dashed curves). For comparison, Fig. 3b depicts the mean latitude of the pixels contributing to the retrievals at a certain scattering angle. In general, one can think of at least two reasons for the observed variability. First, some of the AOT variations may reflect real spatial patterns in the global AOT fields that are imprinted on the scattering-angle dependence due to the fact that the predominant angle at which a location is observed is a function of latitude. Second, scattering- and view-angle biases caused by using inappropriate aerosol and/or surface models in the retrieval algorithm can be expected and are likely to have land surface type, regional, and seasonal dependencies [27,33–36] that make their diagnosis and disentanglement from sampling effects problematic.

One may expect that the dependence on the scattering angle for small AOTs is caused mainly by imperfect assumptions about surface reflectivity in the retrieval algorithm, since the contribution of aerosols to the total signal is relatively small. We may thus conclude from the flatness of the corresponding curves for both land and ocean that surface reflectivity errors alone may not be sufficient to explain the observed all-AOT dependence on the scattering angle.

The latitudinal dependencies (Fig. 3b) for all and small AOTs are similar in shape and exhibit some correlation with the AOT curves in Fig. 3a, thereby suggesting that, indeed, to some extent the AOT variations with the scattering angle may reflect the real world aerosol distribution. At the same time, there are regions where the dominant latitude depends feebly on the scattering angle, and yet large variations are seen in the AOT over both land and ocean. Thus the above qualitative analysis

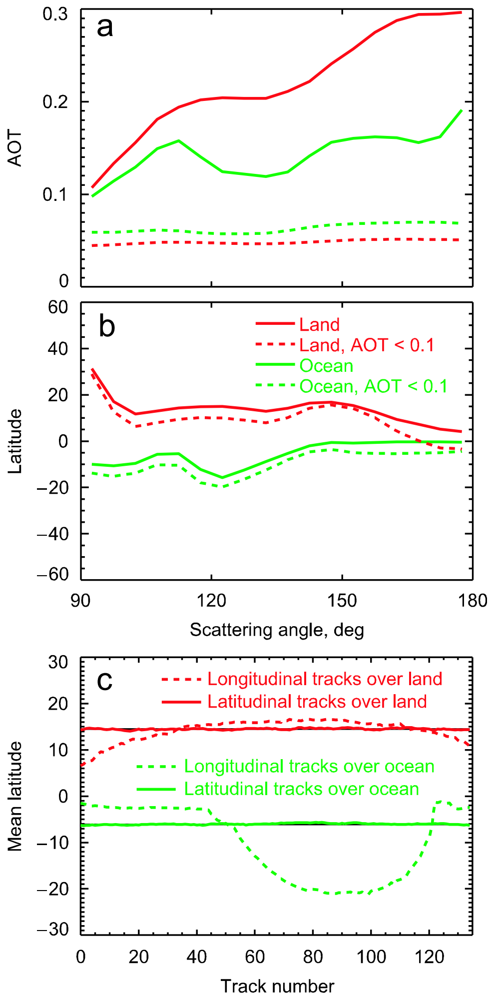

Fig. 3. (a) Variation of MODIS AOTs at 550 nm with scattering angle. (b) Mean latitude of MODIS pixels contributing to the retrievals with a given scattering angle. (c) Mean latitude of global longitudinal-track (dashed curves) and latitudinal-track (solid curves) retrievals as functions of the track number. The horizontal black lines indicate the corresponding mean latitudes of the full imager retrievals.

cannot exclude the presence of angular biases in the MODIS AOT data. MODIS aerosol-product biases over land were analyzed using AERONET data in Ref. [27]. Dependencies similar to the ones presented in Fig. 3a and b were analyzed in Ref. [16].

For the statistical analysis of likely implications of single-track sampling in climate applications, these biases are important only to the extent of being different for different longitudinal tracks and thus potentially being misinterpreted as representing actual statistical variability of the AOT field. It is fundamentally important, however, that one can expect the latitudinal-track sampling to have exactly the same angular biases as the imager data while being as representative statistically as the longitudinal-track sampling. One can thus expect the latitudinal-track statistics to be especially effective in separating the instrumental and sampling effects when comparing single-track and full imager data.

Fig. 4 shows the variation of the global mean AOT as a function of the longitudinal or latitudinal track number (cf. Figs. 1 and 2). We calculated the ratio of the global mean for each longitudinal track (solid curves) and latitudinal track (dot–dashed curves) to the full-imager mean for each month. We then plotted their median values over all months as a function of the track number.

It should be recognized that there may be too few or no data from a given virtual single-track instrument for some of the 10° by 10° grid cells where the imager data are available. In particular over ocean a whole belt of geographic latitudes is absent for tracks affected by the sunglint. To account for this geographic coverage difference between the single-track instruments and the imager, the global imager mean was calculated using only the grid cells where data for the given track are present. To illustrate the magnitude of the geographic coverage effect of the glint on various MODIS tracks, the upper panel of Fig. 4 also shows the same longitudinal-track ratio calculated with all imager data included (dashed curve). The longitudinal-track values show deviations from the imager mean reaching 15% over land and exceeding 20% over ocean. The overall patterns are different over land and ocean: the former exhibits a symmetric dependence on the track number with respect to nadir, whereas the latter is asymmetric, the geographical effects of the glint being apparent from the large differences between the two ratios for the glint-affected tracks. On the other hand,

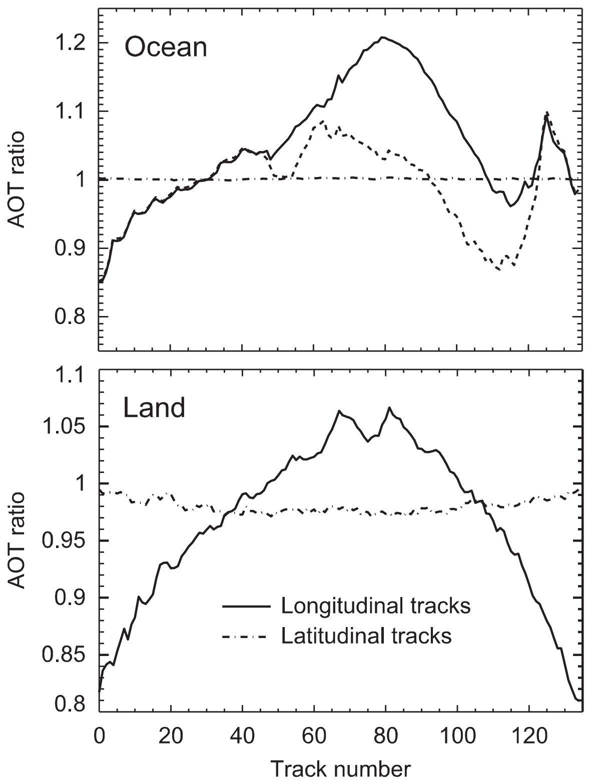

Fig. 4. Median over all months of the ratio of longitudinal-track (solid curves) and latitudinal-track (dot–dashed curves) global monthly mean AOTs at 550 nm to the corresponding imager monthly means over ocean and land. See main text for an explanation of the dashed curve.

for the tracks not affected by the glint the two ratios match closely. Individual months and years exhibit variations of similar magnitude, although the pattern of AOT variations of longitudinal-track samples may change.

The latitudinal-track samples show much less variability than the longitudinal-track ones, thereby suggesting that, indeed, in terms of angular artifacts they mimic closely the original imager data. Their dependence on the track number is flat, consistent with the random way they were constructed. The latitudinal-track variability is somewhat stronger over land than over ocean, which may be an artifact of the smaller data volume.

Fig. 3c shows the median of the mean latitude of the pixels that contributed to the global mean of each virtual instrument as a function of the track number. Solid black curves indicate the mean imager latitude values. One can see that the mean latitude is essentially the same for all latitudinal tracks, thus indicating that they match the geographical coverage of the imager very well. The large dip of the longitudinal-track curve over ocean is the result of the exclusion of certain latitudes for the tracks affected by the glint. Over land, the mean latitude for the outmost longitudinal MODIS tracks begins to diverge from the imager value, which may be an indication of the difficulty of aerosol retrieval at these geometries and hence reduced geographic coverage.

Given a set of longitudinal- and latitudinal-track samples for each value of the global monthly mean AOT, we calculate longitudinal-track and latitudinal-track standard errors. We use all 135 samples to calculate the latitudinal-track standard error. Over land, all 135 tracks are also used to find the longitudinal-track values. Because of the strong influence of the sunglint on the geographic coverage of some tracks, we calculate the longitudinal-track standard error over ocean using the tracks unaffected by the glint, specifically tracks 1–45 and 125–135. The results are presented in Fig. 5 where time series of monthly AOT imager means over ocean and land are shown by solid curves. Longitudinal-track and latitudinal-track standard errors are shown as lightly and darkly shaded areas around the imager mean. Each area represents plus-or-minus three standard errors.

To provide an estimate of the effect that geographic exclusion due to the sunglint has on the longitudinal-track variability we note that the standard error calculated using all longitudinal MODIS tracks over ocean (not shown in Fig. 5) is on average twice as large and has a visible seasonality with the maximum in the summer.

In the absence of any viewing geometry artifacts the longitudinal-track and latitudinal-track standard errors should be of roughly the same magnitude. One can see however from Fig. 5 that the latitudinal-track variability is much smaller than the longitudinal-track one over both land and ocean. On average over the ocean latitudinal-track standard error is 85% less than the longitudinal-track one (absolute values 0.0012 versus 0.0079), and over land it is about one third of the longitudinal-track error (absolute values 0.0054 versus 0.0188). This implies that viewing geometry is the most important contributor to the retrieved MODIS AOT variability, especially over the ocean.

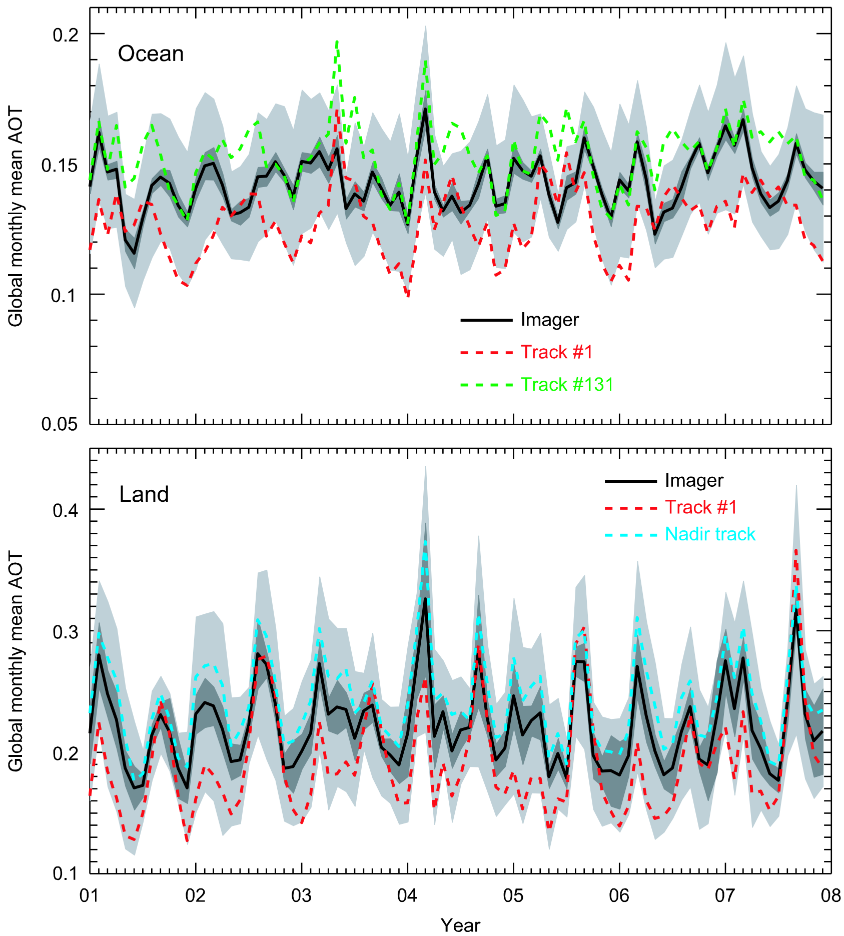

Fig. 5. (a) Time series of global monthly mean AOT over ocean. Lightly and darkly shaded areas represent three longitudinal-track and latitudinal-track standard errors around the full-imager mean, respectively. Dashed curves indicate the means for the first and 131st longitudinal tracks. (b) Time series of global monthly mean AOT over land. Lightly and darkly shaded areas represent three longitudinal-track and latitudinal-track standard errors around the imager mean respectively. Dashed curves indicate the means for the first and the nadir longitudinal tracks.

Also shown in Fig. 5 are the means for three individual longitudinal tracks (dashed curves). Over ocean, we chose to show the tracks on the two sides of the glint-affected area (1st and 131st). Over land, the 1st and the nadir tracks are shown. These particular tracks were chosen to reflect the range of observed track-to-track variability (cf. Fig. 4). As expected, differences between the individual longitudinal tracks are comparable to the 3-standard-errors envelope. One can also notice that values for one of the tracks shown are systematically higher than those for the other. This suggests that part of the longitudinal-track variability is not random but rather is a result of a deterministic dependence on the viewing geometry. A larger footprint for the off-nadir tracks may also contribute to the difference.

Fig. 6 illustrates the geographic AOT distribution of the observed effects. Panel (a) shows the mean imager AOT over land and ocean for the year 2007. Panel (c) shows the absolute AOT difference between the annual mean for one latitudinal track and the imager mean for the same year. Similarly, panels (b) and (d) display the differences between longitudinal-track and full-imager annual means. We use the same individual tracks as in Fig. 5, viz., panel (b) uses the 131st longitudinal track over ocean and the nadir track over land while panel (d) uses the 1st longitudinal track over both ocean and land. To make the maps in panels (b) and (c) representative of the annual differences and to exclude outliers, we require that at least 2000 individual pixel values contribute to each gridbox.

The differences between the latitidinal-track and full-imager gridbox means are on the order of 0.01 over ocean and are distributed fairly uniformly, while over land they are somewhat greater and can reach 0.025 for some gridbox annual means. Other latitudinal-track means exhibit very similar geographic distributions and are, therefore, not shown.

As can be seen from the right-hand panels of Fig. 6, the differences between single longitudinal-track and imager means can be significantly larger. They exceed 0.05 for track 131 (panel (b)) in the Saharan dust outflow region and can fall below −0.05 for some gridboxes in the Southern Ocean. Comparison of panels (b) and (d) also shows that, unlike the situation with the latitudinal tracks, the magnitude and geographic distribution of the longitudinal-track differences

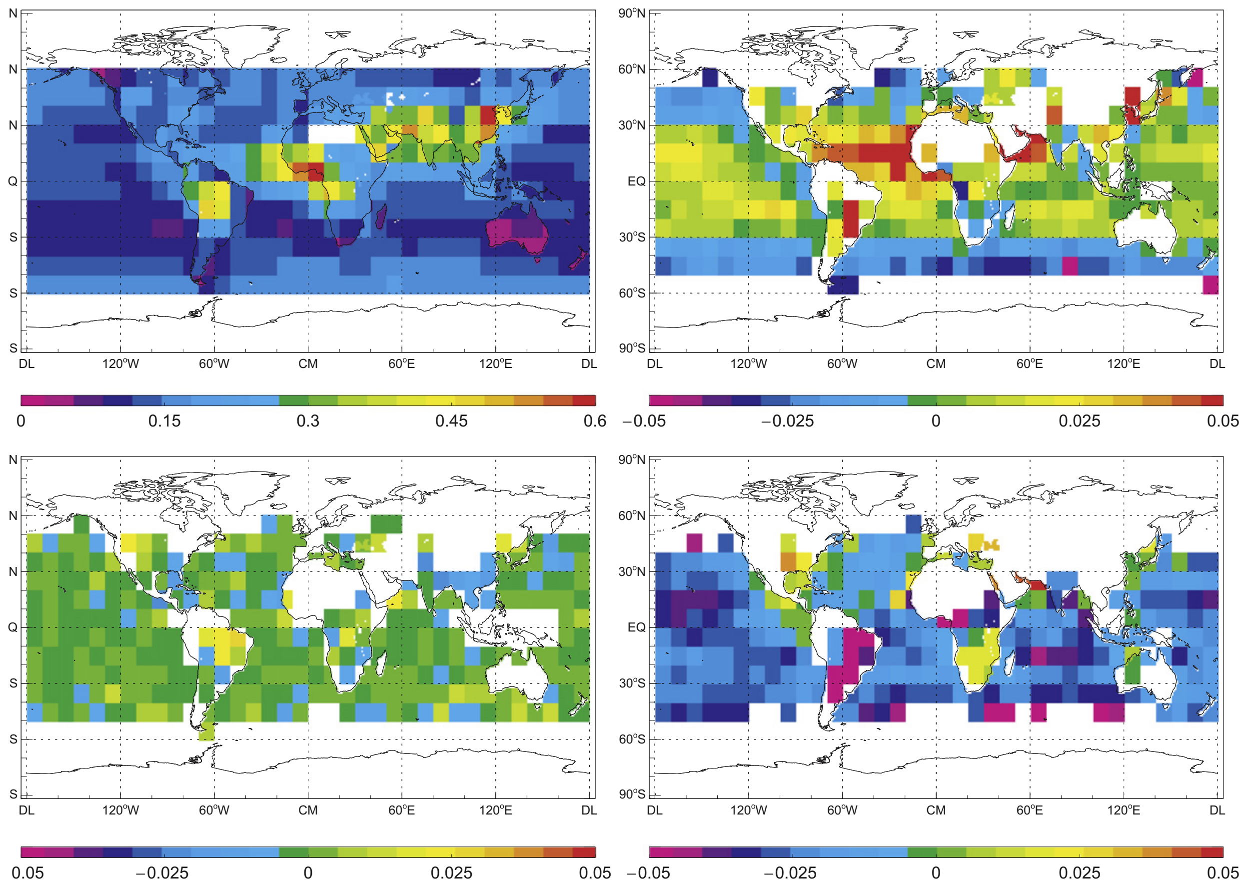

Fig. 6. (a) Mean full-imager AOT for 2007. (b) AOT difference between single-track and full-imager annual means for 2007. Longitudinal track 131 is used over ocean and the nadir track over land. (c) AOT difference between single latitudinal-track and full-imager annual means for 2007. (d) As in (b), but for longitudinal track 1.

vary from track to track. For example, over large areas in the Pacific, track 131 data generally exceed those of the full imager by more than 0.02, while those of track 1 fall below by the same amount. The discrepancies are even larger over some land areas: for a region in South America, the nadir-track and track 1 data differ by more than 0.12 in annual means, thereby strongly indicting the presence of track-to-track artifacts. Comparison of panels (b) and (d) with panel (c) shows that differences between the single-track and full-imager results become smaller and more geographically uniform if one switches from longitudinal-track to latitudinal-track sampling, both regionally and globally.

4. Discussion

Figs. 5 and 6 suggest that using longitudinal-track subsets of MODIS AOTs directly to analyze the sampling adequacy of single-track instruments can lead to false conclusions owing to the apparent enhancement of natural aerosol variability by the track-to-track artifacts. This is the main criticism that we have of the analysis presented in Ref. [37]. The analysis based on the statistics of the latitudinal-track means yields better estimates because it allows for better separation of the viewing-geometry artifacts and true natural variability.

One should recognize that it may be impossible to determine without invoking external datasets to what extent the smaller latitudinal-track standard error is controlled by the natural aerosol variability and how much it is contributed to by potential instrumental and retrieval errors. We can therefore consider it to be the upper limit of AOT errors caused by an along-track instrument under the assumption that the imager-retrieved values represent "true" global monthly means. It is quite likely that improved retrieval capabilities of along-track instruments such as APS or CALIOP will reduce the error estimate even further.

Hansen et al. [38] estimated that a global AOT change of 0.01 would yield a climatically important flux change of 0.25 W/m^2. Based on a model perturbation analysis, Loeb and Su [3] arrived at similar values of the direct radiative forcing for a 0.01 change in the global AOT assuming that the other aerosol parameters remain fixed. Since the standard error estimates that we have obtained are comfortably below 0.01, we may conclude that along-track instruments flown on a sun-synchronous orbiting platform have sufficient spatial sampling for estimating aerosol effects on climate. One of the advantages of APS-like polarimeters is a much improved sensitivity to aerosol composition parameters such as complex refractive index, size distribution, and nonsphericity. A lidar can provide an accurate estimate of aerosol vertical distribution. These climatically-important parameters are believed to be less variable than the AOT and are therefore even less demanding in terms of sampling density.

One of the anonymous reviewers of this paper suggested that the radiance calibration degradation of the MODIS Terra instrument and specifically the issue of response versus scan (RVS) may have affected the view-angle bias of AOT retrievals in Collection 5 [39]. This effect is estimated to be much smaller in MODIS Aqua data and is planned to be rectified in Collection 6. It is therefore possible that for MODIS Aqua AOTs, the standard error growth when switching from latitudinal- to longitudinal-track subsampling will be smaller. Note, however, that for the 7-year period studied in this paper the MODIS Terra data do not show any apparent changes in the relative magnitude of the longitudinal-track versus latitudinal-track variability. This implies that the MODIS Terra RVS degradation may not have been the only contributor to the observed track-to-track biases in AOT. Clearly, this issue requires further analysis. However, for the purpose of single-track sampling evaluation the analysis presented here demonstrates that the latitudinal-track approach is sufficiently robust to be useful even with the less-than-perfect MODIS Terra data.

5. Conclusions

Owing to its global coverage, longevity, and extensive characterization versus ground-based data, the MODIS level-2 aerosol product is an instructive testbed for assessing sampling effects on climatic means derived from along-track instrument data. The presence of track-to-track artifacts in longitudinal strips of MODIS data makes it unsuitable for estimating the *lower limit* of errors caused by pixel-wide along-track sampling. On the other hand, these very artifacts make the MODIS AOT dataset a reliable tool for estimating the *upper limit* of such errors.

Our analysis shows that using individual longitudinal MODIS tracks directly can significantly overestimate errors of an along-track instrument because of the exaggeration of apparent AOT variability by MODIS track-to-track angular biases. Using latitudinal-track samples of MODIS AOTs yields much more reliable estimates of sampling-caused errors of an along-track instrument. Based on published assessments of aerosol effects on climate, we conclude that along-track instruments such as CALIOP and APS should have sufficient coverage for climate applications.

Our findings are important given the greater ability of along-track instruments to retrieve a wider range of aerosol properties needed for modeling climate and climate change. We believe that the proposed methodology can be used in analyses of along-track sampling effects on the retrieval of other atmospheric variables based on imperfect imager data.

Acknowledgments

We thank Li Liu for help with MODIS level-2 data and two anonymous reviewers whose insightful comments resulted in a much improved manuscript. This study was supported by the research division of the NASA Glory Mission Project managed by Hal Maring.

References

[1] IPCC Summary for Policymakers. In: Solomon S, Qin D, Manning M, Chen Z, Marquis M, Averyt KB, Tignor M, Miller HL, editors. Climate change 2007: the physical science basis. Cambridge, UK: Cambridge Univ. Press; 2007.
[2] Kiehl JT. Twentieth century climate model response and climate sensitivity. Geophys Res Lett 2007;34:L22710.
[3] Loeb NG, Su W. Direct aerosol radiative forcing uncertainty based on a radiative perturbation analysis. J Climate 2010;23:5288–93.
[4] Lohmann U, Ferrachat S. Impact of parametric uncertainties on the present-day climate and on the anthropogenic aerosol effect. Atmos Chem Phys 2010;10:11373–83.
[5] Penner JE, Xu L, Wang M. Satellite methods underestimate indirect climate forcing by aerosols. Proc Natl Acad Sci USA 2011;108: 13404–8.
[6] Hansen J, Sato M, Kharecha P, von Schuckmann K. 2011: Earth's energy imbalance and implications. Atmos Chem Phys 2011;11: 13421–49.
[7] King MD, Menzel WP, Kaufman YJ, Tanré D, Gao BC, Platnick S, et al. Cloud and aerosol properties, precipitable water, and profiles of temperature and water vapor from MODIS. IEEE Trans Geosci Remote Sens 2003;41:442–58.
[8] Remer L, Kleidman RG, Levy RC, Kaufman YJ, Tanré D, Mattoo S, et al. Global aerosol climatology from the MODIS satellite sensors. J Geophys Res 2008;113:D14S07.
[9] Levy RC. The dark-land MODIS collection 5 aerosol retrieval: algorithm development and product evaluation. In: Kokhanovsky AA, de Leeuw G, editors. Satellite aerosol remote sensing over land. Chichester, UK: Praxis; 2009. p. 19–68.
[10] Diner D, Beckert J, Reilly T, Bruegge CJ, Conel JE, Kahn RA, et al. Multiangle imaging sptectrradiometer (MISR) description and experiment overview. IEEE Trans Geosci Remote Sens 1998;36: 1072–87.
[11] Martonchik JV, Diner DJ, Crean KA, Bull MA. Regional aerosol retrieval results from MISR. IEEE Trans Geosci Remote Sens 2002;40:1520–31.
[12] Martonchik JV, Kahn RA, Diner DJ. Retrieval of aerosol properties over land using MISR observations. In: Kokhanovsky AA, de Leeuw G, editors. Satellite aerosol remote sensing over land. Chichester, UK: Praxis; 2009. p. 267–293.
[13] Tanré D, Bréon FM, Deuzé YJ, Dubovik O, Ducos F, François V, et al. Remote sensing of aerosols by using polarized, directional and spectral measurements within the A-Train: the PARASOL mission. Atmos Meas Tech 2011;4:1383–95.
[14] Winker DM, Pelon J, Coakley Jr. JA, Ackerman SA, Charlson RJ, Colarco PR, et al. The CALIPSO mission: a global 3D view of aerosols and clouds. Bull Am Meteorol Soc 2010;91:1211–29.
[15] Mishchenko MI, Cairns B, Kopp G, Schueler CF, Fafaul BA, Hansen JE, et al. Accurate monitoring of terrestrial aerosols and total solar irradiance: introducing the Glory Mission. Bull Am Meteorol Soc 2007;88:677–91.
[16] Cairns B, Mishchenko MI, editors. New York: NASA Goddard Institute for Space Studies; 2012. 〈http://glory.giss.nasa.gov/APS-2_Report.pdf〉.
[17] Knobelspiesse K, Cairns B, Mishchenko M, Chowdhary J, Tsigaridis K, van Diedenhoven B, et al. Analysis of fine-mode aerosol retrieval capabilities by different passive remote sensing instrument designs. Opt Exp 2012;20:21457–84.
[18] Mishchenko MI, Cairns B, Hansen JE, Travis L, Burg R, Kaufman Y, et al. Monitoring of aerosol forcing of climate from space: analysis of measurement requirements. J Quant Spectrosc Radiat Transfer 2004;88:149–61.
[19] Ichoku C, Remer LA, Eck TF. Quantitative evaluation and intercomparison of morning and afternoon moderate resolution imaging spectroradiometer (MODIS) aerosol measurements from Terra and Aqua. J Geophys Res 2005;110:D10S03.
[20] Remer L, Kaufman Y, Tanré D, Mattoo S, Chu D, Martins J, et al. The MODIS aerosol algorithm, products and validation. J Atmos Sci 2005;62:947–73.
[21] Kahn R, Gaitley R, Martonchik J, Diner D, Crean K, Holben B. MISR global aerosol optical depth validation based on two years of

coincident AERONET observations. J Geophys Res 2005;110: D10S04.

[22] Kahn R, Nelson D, Garay M, Levy R, Bull M, Diner D, et al. MISR aerosol product attributes and statistical comparisons with MODIS. IEEE Trans Geosci Remote Sens 2009;47:4095–114.

[23] Chýlek P, Henderson BG, Lesins G. Aerosol optical depth retrieval over the NASA Stennis Space Center: MTI, MODIS, and AERONET. IEEE Trans Geosci Remote Sens 2005;43:1978–83.

[24] Xiao N, Shi T, Calder CA, Munroe DK, Berrett C, Wolfinbarger S, et al. Spatial characteristics of the difference between MISR and MODIS aerosol optical depth retrievals over mainland Southeast Asia. Remote Sens Environ 2009;113:1–9.

[25] Mishchenko MI, Geogdzhayev IV, Liu L, Lacis AA, Cairns B, Travis LD. Toward unified satellite climatology of aerosol properties: what do fully compatible MODIS and MISR aerosol pixels tell us? J Quant Spectrosc Radiat Transfer 2009;110:402–8.

[26] Mishchenko MI, Liu L, Geogdzhayev IV, Travis LD, Cairns B, Lacis AA, et al. Toward unified satellite climatology of aerosol properties. 3. MODIS versus MISR versus AERONET. J Quant Spectrosc Radiat Transfer 2010;111:540–52.

[27] Levy RC, Remer LA, Kleidman RG, Mattoo S, Ichoku C, Kahn R, et al. Global evaluation of the Collection 5 MODIS dark-target aerosol products over land. Atmos Chem Phys 2010;10:10399–420.

[28] Shi Y, Zhang J, Reid JS, Holben B, Hyer EJ, Curtis C. An analysis of the collection 5 MODIS over-ocean aerosol optical depth product for its implication in aerosol assimilation. Atmos Chem Phys 2011;11: 557–65.

[29] Holben BN, Eck TF, Slutsker I, Tanré D, Buis JP, Setzer A, et al. AERONET—a federated instrument network and data archive for aerosol characterization. Remote Sens Environ 1998;66:1–16.

[30] Dubovik O, Holben B, Eck TF, Smirnov A, Kaufman YJ, King M, et al. Variability of absorption and optical properties of key aerosol types observed in worldwide locations. J Atmos Sci 2002;59:590–608.

[31] Kinne S, Schulz M, Textor C, Guibert M, Balkanski Y, Bauer SE, et al. An AeroCom initial assessment – optical properties in aerosol component modules of global models. Atmos Chem Phys 2006;6: 1815–34.

[32] Shindell D, Faluvegi G. Climate response to regional radiative forcing during the twentieth century. Nature Geosci 2009;2: 294–300.

[33] Remer L, Ward AE, Kaufman YJ. Angular and seasonal variation of spectral ratios: implications for the remote sensing of aerosol over land. IEEE Trans Geosci Remote Sens 2001;39:275–83.

[34] Gatebe CK, King MD, Tsay S, Ji Q, Arnold GT, Li JY. Sensitivity of off-nadir zenith angles to correlation between visible and near-infrared reflectance for use in remote sensing of aerosol over land. IEEE Trans Geosci Remote Sens 2001;39:805–18.

[35] Mishchenko MI, Geogdzhayev IV, Liu L, Ogren JA, Lacis AA, Rossow WB, et al. Aerosol retrievals from AVHRR radiances: effects of particle nonsphericity and absorption and an updated long-term global climatology of aerosol properties. J Quant Spectrosc Radiat Transfer 2003;79–80:953–72.

[36] Herman M, Deuzé JL, Marchant A, Roger B, Lallart P. Aerosol remote sensing from POLDER/ADEOS over the ocean: improved retrieval using a non-spherical particle model. J Geophys Res 2005;110: D10S02.

[37] Colarco PR, Remer LA, Kahn RA, Levy RC, Welton EJ. Implications of satellite swath width on global aerosol optical thickness statistics. Atmos Meas Tech Discuss 2012;5:2795–820.

[38] Hansen J, Rossow W, Carlson B, Lacis A, Travis L, Del Genio A, et al. Low-cost long-term monitoring of global climate forgings and feedbacks. Climate Change 1995;31:247–71.

[39] Meister G, Franz BA, Kwiatkowska EJ, McClain CR. Corrections to the calibration of MODIS Aqua ocean color bands derived from SeaWiFS data. IEEE Trans Geosci Remote Sens 2012;50:310–9.